ELSEVIER

A comparative study of quantum yield and electrical energy per order (E_{Eo}) for advanced oxidative decolourisation of reactive azo dyes by UV light

M. Muruganandham [a,1], K. Selvam, M. Swaminathan [a,*]

[a] *Department of Chemistry, Annamalai University, Annamalai Nagar, India*

Abstract

This paper evaluates the quantum yield and electrical energy per order (E_{Eo}) efficiency of Reactive Orange 4 (RO4) and Reactive Yellow 14 (RY14) azo dyes by three advanced oxidation processes (AOPs). Both dyes were completely decolourised by all these processes. The relative decolourisation efficiencies of these processes were in the following order: $Fe^{2+}/H_2O_2/UV > UV/TiO_2 > UV/H_2O_2$. The low efficiency of UV/H_2O_2 process is mainly due to low UV absorption by hydrogen peroxide at the 365 nm. The figure of merit E_{Eo} values showed that UV/H_2O_2 process consumes more electrical energy than the other two processes. The electrical energy consumption is in the following order: $UV/H_2O_2 > UV/TiO_2 > Fe^{2+}/H_2O_2/UV$. At low initial dye concentration higher quantum yield was observed in UV/TiO_2 process, whereas in photo-Fenton process higher quantum yield was observed at high initial dye concentration. The structure of dye molecule also influences the quantum yield and E_{Eo} value.
© 2006 Published by Elsevier B.V.

Keywords: Advanced oxidation processes; Quantum yield; Electrical energy per order; Decolourisation; UV-A light; Reactive dyes

1. Introduction

Environmental concerns have led to extensive research on the removal of harmful organic compounds from industrial waste stream. The uncontrolled release of coloured dye effluent from textile and other colour industries into the environment causes many ecological problems. An inexpensive and versatile solution, especially for wastewater discharged from textile industries, has not yet been developed. Nowadays, reactive dyes are widely used in the textile industry because of their good colour fixation due to the covalent bond formation with natural (or) synthetic fibers. However, substantial amount of unfixed dyes are lost in the industrial effluent and it is not possible to recover them for reuse because they are chemically modified.

Advanced oxidation processes (AOPs) have been proposed in recent years as an attractive alternative for the treatment of contaminated ground, surface and wastewater containing non biodegradable organic pollutants. The most commonly used AOPs utilised H_2O_2, O_3, O_2, and iron salts as oxidants. Among AOPs, the combined systems UV/TiO_2, UV/H_2O_2, and $UV/Fe^{2+}/H_2O_2$ (photo-Fenton process) are considered as the most promising for the remediation of contaminated waters. All these processes produce OH radicals, which are highly reactive species ($E_O = 2.8\,eV$). They attack most of the organic compounds with a rate constant usually in the order of $106–109\,M^{-1}\,s^{-1}$. Hydroxyl radicals can be generated by a semiconductor photocatalyst on irradiation with UV light. The photocatalyst Titanium dioxide (TiO_2) is a wide band gap semiconductor (3.2 eV) and is successfully used as a photocatalyst for the treatment of organic [1,2] and dye pollutants [3–6].

For the decolourisation studies in UV/TiO_2 process, we have used suspension type photocatalytic reactor. Since the TiO_2 particles may be recovered from the purified wastewater by solid/liquid separation techniques, a suspension reactor has a definite advantage over a fixed photocatalytic reactor because of the latter's limiting mass transfer and the loss of photocatalytic activity due to the fixation of the catalysts. Use of oxygen from air as the electron acceptor reduces the recombination of the electron/hole pair and increases the photonic efficiency. The photo-Fenton reaction is known to be a most promising process
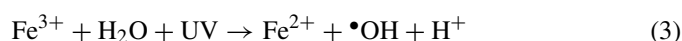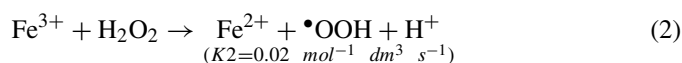
* Corresponding author. Tel.: +91 4144 220572.
  E-mail address: chemsam@yahoo.com (M. Swaminathan).
[1] Present address: Department of Environmental Engineering and Science, Feng Chia University, Taichung, Taiwan.

for the remediation of highly contaminated waters. Hydrogen peroxide in the presence of Fe^{2+} produces reactive hydroxyl radical under acidic condition according to Eq. (1).

$$Fe^{2+} + H_2O_2 \rightarrow {}^{\bullet}OH + Fe^{3+} + OH^- \qquad (1)$$
$$(K1 = 58 \ mol^{-1} \ dm^3 \ s^{-1})$$
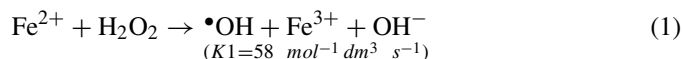
The reagent components are easy to handle and environmentally harmless making this system attractive for treating aqueous contaminants. The Fe^{3+} produced in Eq. (1) further reacts with H_2O_2, H_2O to regenerate Fe^{2+} as represented in Eqs. (2) and (3). The generated Fe^{3+} undergoes spontaneous hydrolysis with water and form several species, mainly the monohydroxy complex $Fe(OH)^{2+}$ at pH 3.0. This species is capable of producing Fe^{2+} and hydroxyl radical directly by the photolysis under UV–vis irradiation (Eq. (4)). The combined photo-Fenton process ((1)–(4)) accelerates strongly the rate of degradation of organic compounds when compared to the Fenton process. This photo-Fenton process had been extensively used to degrade the pollutants [7–10,18].

$$Fe^{3+} + H_2O_2 \rightarrow Fe^{2+} + {}^{\bullet}OOH + H^+ \qquad (2)$$
$$(K2 = 0.02 \ mol^{-1} \ dm^3 \ s^{-1})$$

$$Fe^{3+} + H_2O + UV \rightarrow Fe^{2+} + {}^{\bullet}OH + H^+ \qquad (3)$$

$$Fe(OH)^{2+} + UV \rightarrow Fe^{2+} + {}^{\bullet}OH \qquad (4)$$

During the last decade, some investigations have been reported about the successful application of UV/H_2O_2 process for dye wastewater treatment. In UV/H_2O_2 process, the photolysis of hydrogen peroxide generates effective oxidising species hydroxyl radical (${}^{\bullet}OH$) according to Eq. (5).

$$H_2O_2 + UV \rightarrow {}^{\bullet}OH + {}^{\bullet}OH \qquad (5)$$

Hydrogen peroxide with UV light has been found to be very effective in the degradation of dye pollutants [11–14]. The complete decolourisation and mineralisation of dyes by UV radiation in the presence of H_2O_2 have also been reported [15,16]. In addition, UV/H_2O_2 process has several advantages over other AOPs:

(i) there is no sludge formation during the treatment; (ii) it can be carried out under ambient conditions; (iii) the oxygen formed in this process is also useful for aerobic biological decay process [17].

The main objective of this paper is to evaluate the efficiencies of the decolourisation of Reactive Orange 4 (RO4) and Reactive Yellow 14 (RY14) by these three AOPs. Performance of the treatment systems has been assessed on the basis of quantum efficiency and electrical energy per order (E_{Eo}).

2. Experimental

2.1. Materials

RO4 and RY14 dyes obtained from Colour Chem., Pondicherry were used as received. The chemical formulas of RO4 dye (CI. No. 18260, molecular formula = $C_{23}H_{13}N_6O_{10}S_3C_{12}Na_3$, molecular weight = 769.21, absorption maxima = 489 nm) and RY14 (C.I. No.19036, molecular formula = $C_{20}H_{19}N_4O_{11}S_3Na_2Cl$, molecular weight = 669.00, absorption maxima = 410 nm) are shown in Fig. 1. A gift sample of TiO_2-P25 was received from Degussa (Frankfurt, Germany). TiO_2-P25 contains Anatase 80% and Rutile 20% with the mean particle size of 30 nm and a BET surface area of 50 m^2/g. AnalaR grade reagents H_2O_2 (30%, w/w) and FeSO4·7H2O were used as received. The double distilled water was used to prepare experimental solutions. The pH of the solutions was adjusted using H_2SO_4 or NaOH.

2.2. Apparatus

Heber multilamp photoreactor model HML-MP 88 was used for photoreaction. This model consists of eight medium-pressure Mercury vapor lamps of 8 W, each set in parallel, and emitting 365 nm wavelengths. It has a reaction chamber with specially designed reflectors made of highly polished aluminum and built in cooling fan at the bottom. It is provided
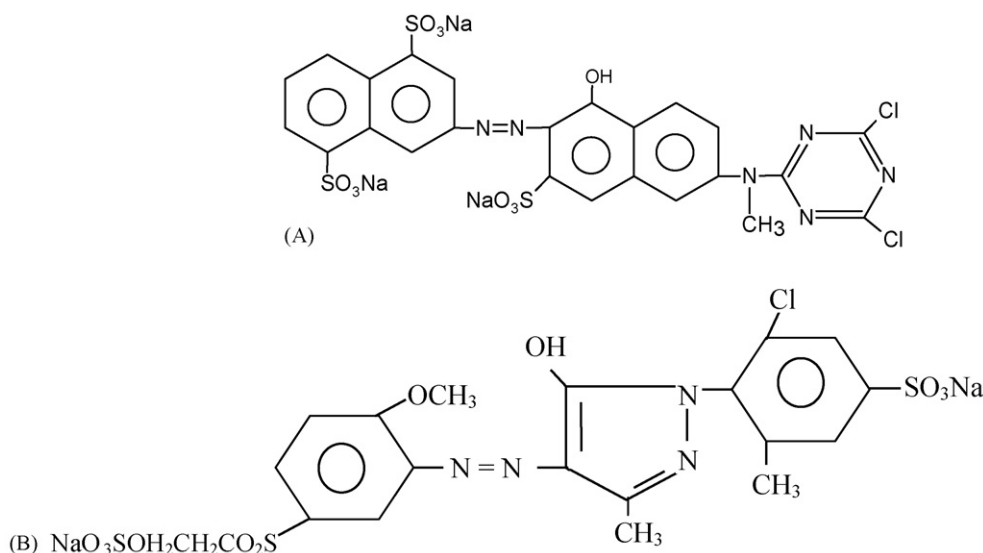

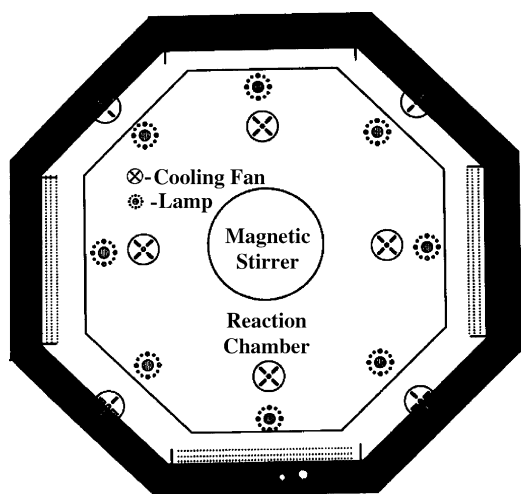Fig. 1. Structure of dye (A) RO4 (B) RY14.

Fig. 2. Schematic diagram of photoreactor.

with the magnetic stirrer at the center. Open borosilicate glass tube of 50 mL capacity, 40 cm height, and 20 mm dia was used as a reaction vessel with the total light exposure length of 330 mm. The irradiation was carried out using four parallel medium-pressure Mercury lamps (32 W) in open-air condition. Heat effect of the lamps during the photoreaction was eliminated and the temperature of the reaction solution was maintained at constant value, $30 \pm 1.0\,^{\circ}C$, by allowing cooled air between the lamps and the reaction solution. The schematic diagram of reactor is shown in Fig. 2. The solution with TiO_2 and dye was continuously aerated by a pump to provide oxygen and for complete mixing of reaction solution. The intensity of irradiation entering the glass tube was measured by potassium ferrioxalate actinometery method. The actinometer solution was irradiated under conditions similar to those used for photoreaction. Light intensity (lo) of four lamps measured using 50 mL of the actinometer solution was 1.38×10^{-06} Einstein $L^{-1}\,s^{-1}$.

2.3. Procedure

50 mL of the dye solution containing appropriate quantity of the TiO_2 suspensions was used for TiO_2 process and the suspension was stirred for 30 min in the dark for the attainment of adsorption equilibrium. At specific time intervals, 2 mL of the sample was withdrawn and centrifuged to separate the catalyst. 1 mL of the centrifugate was diluted to 10 mL and its absorbance at 489 nm for RO4 dye and 410 nm for RY14 dye, were measured. The absorbance at 489 and 410 nm ($n{\rightarrow}\pi^{*}$ transition of –N=N–group) is due to the colour of the dye solution and it is used to monitor the decolourisation of dyes. For UV/H_2O_2 process, a desired molar ratio of dye/H_2O_2 at pH 3 was prepared freshly before the experiments. For Fenton and photo-Fenton process, a desired molar ratio of dye/Fe^{2+}/H_2O_2 solution was freshly prepared from $FeSO_4 \cdot 7H_2O$ and the dye stock solution. The pH of the solution was adjusted to 3.0. (For Fenton process the mixture was kept in the dark.) After irradiation the absorbance was measured immediately to avoid further reaction. The pH of the solution was adjusted to 5.5 before taking the concentration measurements. All the experiments in UV/H_2O_2,

Fenton and photo-Fenton processes were carried out at pH 3.0. For UV/TiO_2 process, the experiments were conducted at the natural pH 5.5 of the solution. The interference by ferrous ions in the UV region was negligible in the concentration range used for the present study. During the illumination time, no volatility of the solvent was observed. UV spectral measurements were done using Hitachi U-2001 spectrophotometer. The pH of the solution is measured by using HANNA Phep (Model H 198107) digital pH meter.

3. Results and discussion

3.1. Decolourisation of RO4 and RY14 by different AOPs

Fig. 3 depicts RO4 and RY14 dye decolourisation by UV/H_2O_2 process as a function of reaction time. Both dyes are resistant to direct photolysis of UV light (data not shown). H_2O_2 with dye in dark causes 2.3 and 3.7% of decolourisation whereas combined action of UV and H_2O_2 causes 47.2 and 34.1% of decolourisation in 40 min for RO4 and RY14 dyes respectively. Both dyes contain one azo bond and decolourisation of dye is due to the initial electrophilic cleavage of its chromophoric azo (–N=N–) bond attached to aromatic ring. Although the removal efficiency of RO4 dye is more efficient than RY14 dye at the initial reaction periods, the removal efficiency is the same at the end of the reaction (after 120 min of irradiation). These results imply that chemical structure of these dyes has not appreciably influenced the overall decolourisation efficiency.

Fig. 4 shows the decolourisation results of photo-Fenton processes (UV/H_2O_2/Fe^{2+}) for both dyes. In order to understand the fate of photo-Fenton process clearly, the decolourisation was also carried out without UV irradiation (Fenton process-H_2O_2/Fe^{2+}) for comparison. In Fenton process, the colour removal is 79.8 and 84.11% in 40 min, whereas for the same time in photo-Fenton process, 95.5 and 94.56% of decolourisation are observed for RO4 and RY14 dyes, respectively. Initially, a large degree of removal is observed for both the dyes and the decolourisation efficiency which is almost the same as in photo-Fenton processes. The high removal rate of photo-Fenton
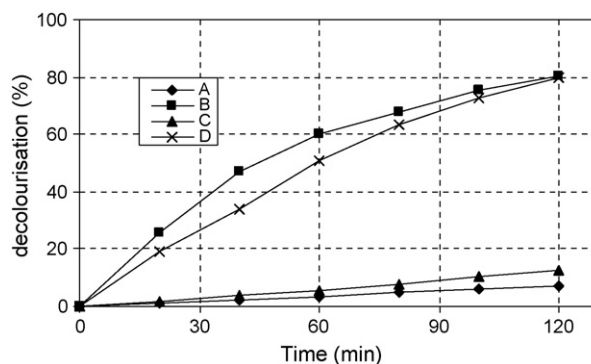

Fig. 3. Decolourisation of RO4 and RY14 by UV/H_2O_2 process. [Dye] = 5×10^{-4} mol/L, [H_2O_2] = 10 mM, pH 3.0, $I_0 = 1.38 \times 10^{-06}$ Einstein $L^{-1}\,S^{-1}$. [A] = RO4 without UV irradiation, [B] = RO4 with UV irradiation, [C] = RY14 without UV irradiation, [D] = RY14 with UV irradiation.
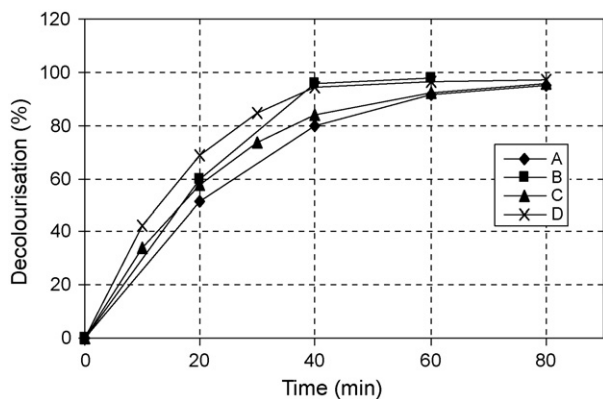
Fig. 4. Decolourisation of RO4 and RY14 by Fenton (H_2O_2/Fe^{2+}) and photo-Fenton (UV/H_2O_2/Fe^{2+}) processes. [Dye] = 5×10^{-4} mol/L, [Fe^{2+}] = 0.05 mM, [H_2O_2] = 10 mM, pH 3.0, $I_0 = 1.38 \times 10^{-06}$ Einstein L^{-1} S^{-1}. [A] = Fenton process of RO4, [B] = photo-Fenton process of RO4, [C] = Fenton process of RY14, [D] = photo-Fenton process of RY14.

process is due to generation of additional hydroxyl radicals by UV-light irradiation.

Fig. 5 depicts photocatalysed decolourisation of RO4 and RY14 as a function of reaction time in UV/TiO_2 process. In the presence of TiO_2 without UV irradiation, about 24.74 and 13.46% of colour removal are observed. This is due to the adsorption of dye molecules on the surface of TiO_2. Simultaneous irradiation of UV light and aeration with TiO_2 caused 85.63 and 91.38% of decolourisation in 40 min for RO4 and RY14, respectively. Adsorption results showed that RO4 dye is more strongly adsorbed on TiO_2 than RY14 dye. RO4 contains three sulphonic groups and hence, in solution it exists as a trianionic species whereas RY14 is present as a dianionic dye. Hence, RO4 is adsorbed more than RY14 dye. However, the decolourisation of RY14 is more than RO4. Generally, at pH <6.8 (point of zero charge (pzc) of TiO_2-P25), a strong adsorption of the dye on the TiO_2 particles is observed as a result of the electrostatic attraction of the positively charged TiO_2 with the anionic dyes which favors the photocatalytic degradation of dye on the surface of TiO_2. However, it is generally believed that the photocatalytic degradation process occurs in the following four
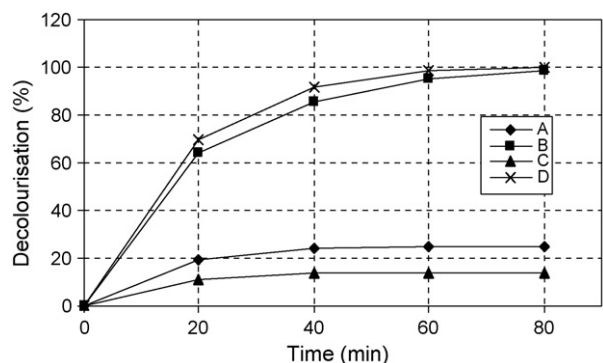
possible ways: (a) the reaction takes place between two adsorbed substances; (b) the reaction occurs between a radical in solution and an adsorbed substrate molecule; (c) the reaction takes place between a radical linked to the surface and a substrate molecule in solution; and (d) the reaction occurs when both radical and substrate are in solution [6]. Our experimental results reveal that the photocatalytic degradation in UV/TiO_2 process occurs both at the surface and in solution. Hence, the effect of dye adsorption on the photocatalytic surface is limited for the decolourisation.

The relative efficiencies of the above processes are in the following order of UV/H_2O_2/Fe^{2+} > UV/TiO_2 > UV/H_2O_2. The differences in decolourisation rate in these processes are mainly due to difference in hydroxyl radical generation in each process. Although a slightly better decolourisation rate was observed in photo-Fenton process, the difference in decolourisation rate between UV/TiO_2 and photo-Fenton processes is not significant. The decolourisation efficiency of UV/H_2O_2 process is quite low when compared to the other two processes. Although hydroxyl radical could be formed in H_2O_2 solution under the irradiation with UV, the decolourisation of RO4 is slow. This could be attributed to the low absorption of H_2O_2 in the range of 300–400 nm. The photolysis of hydrogen peroxide requires $\lambda < 300$ nm as H_2O_2 has a maximum absorption around 250 nm.

3.2. Electrical energy determination

Although several reports are available in the literature on electrical energy determination of various AOPs, it is necessary to study the electrical energy consumption of the AOPs under experimental conditions. Generally, the electrical energy consumption of AOPs depends on number of experimental factors (type of pollutant being treated, configuration of the reactor, and type of light source used, etc.) and hence, electrical energy determination becomes important for the processes studied. A number of important factors such as economics, effluent quality, cost, etc., also play a vital role in selecting a waste treatment technology. Since photodegradation of aqueous organic pollutant is an electrical energy-related process, the electrical energy represents a major fraction of the operating costs. The figures of merit E_{Eo} allows for a rapid determination of the electrical energy cost and they indicate the total power required. For comparative purpose, the treatment efficiencies for the different processes are evaluated through the E_{Eo} values. The E_{Eo} is defined as the number of kWh of electrical energy required to reduce the concentration of pollutant by one order of magnitude (90%) in 1 m^3 of contaminated water. The E_{Eo} values were obtained from the inverse of the slope of a plot of log C/C_0 versus UV dose [19]. Considering first-order degradation kinetics, the UV doses were calculated for all the three AOPs using Eq. (6) [20]. From the UV doses, E_{Eo} can also be calculated using Eq. (7) [19].

Fig. 5. Decolourisation of RO4 and RY14 by UV/TiO_2 process. [Dye] = 5×10^{-4} mol/L, TiO_2 = 4g/l, pH 4.8, $I_0 = 1.38 \times 10^{-06}$ Einstein L^{-1} S^{-1}. [A] = Adsorption of RO4 on TiO_2 surface [B] = UV light irradiation of RO4 in the presence of TiO_2, [C] = Adsorption of RY14 on TiO_2 surface, [D] = UV light irradiation of RY14 in the presence of TiO_2.

$$\text{UV dose} = \frac{\text{Lamp power(kW)} \times \text{Time (h)} \times 1000}{\text{Treated volume (l)}} \quad (6)$$
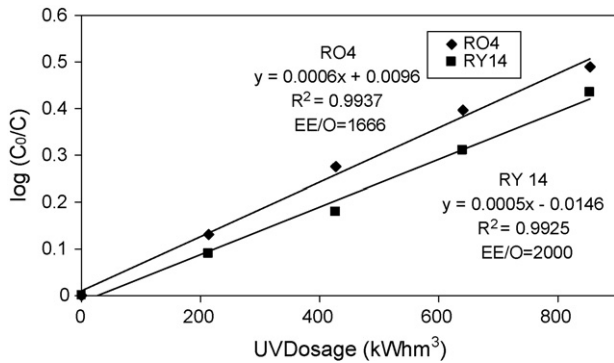
$$E_{Eo} = \frac{\text{UV dose}}{\log C_0/C} \quad (7)$$

Fig. 6. E_{Eo} determination for decolourisation of RO4 and RY14 by UV/H_2O_2 process. [Dye] = 5×10^{-4} mol/L, [H_2O_2] = 10 mM, pH 3.0, $I_0 = 1.38 \times 10^{-06}$ Einstein L^{-1} S^{-1}.
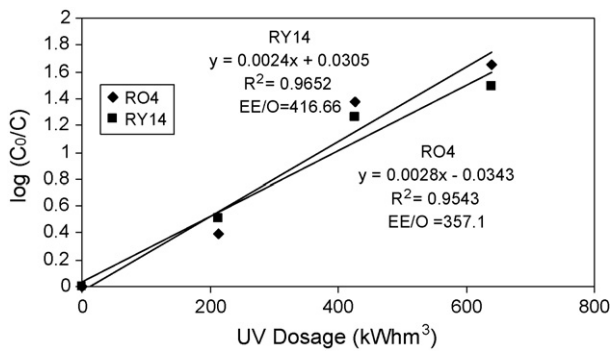

Fig. 7. E_{Eo} determination for decolourisation of RO4 and RY14 by UV/H_2O_2/Fe^{2+} process. [Dye] = 5×10^{-4} mol/L, [Fe^{2+}] = 0.05 mM, [H_2O_2] = 10 mM, pH 3.0, $I_0 = 1.38 \times 10^{-06}$ Einstein L^{-1} S^{-1}.

The UV doses were determined for the light source of 32 W and total volume of 50 mL at different reaction times. The results are presented in Figs. 6–8. UV/H_2O_2 process consumes 1666 and 2000 kWh/m^3 for the complete degradation of 5×10^{-4} mol/L of RO4 and RY14, respectively, whereas photo-Fenton process consumes 357.1 and 416.6 kWh/m^3 for the same concentration of RO4 and RY14. In the case of UV/TiO_2 process, the E_{Eo} values for complete degradation of RO4 and RY14 (5×10^{-4} mol/L) are 500 and 344.8 kWh/m^3. UV/H_2O_2 pro-
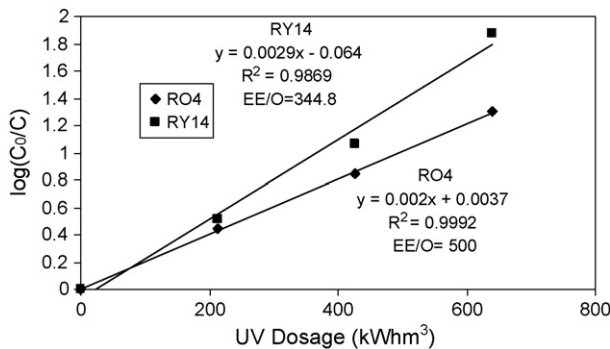

Fig. 8. E_{Eo} determination for decolourisation of RO4 and RY14 by UV/TiO_2 process. [Dye] = 5×10^{-4} mol/L, [TiO_2] = 4 g/l, pH 4.8, $I_0 = 1.38 \times 10^{-06}$ Einstein L^{-1} S^{-1}.

cess requires 4.66 and 3.32-fold more electrical energy than photo-Fenton and UV/TiO_2 processes, respectively, for complete degradation of RO4. Similarly, in RY14 dye, 4.80 and 5.81-fold more electric energy is consumed for UV/H_2O_2 when compared to photo-Fenton and UV/TiO_2 processes. The difference in electrical energy consumption between these two dyes may be due to basic structural difference. From the figures of merit it is very clear that UV/H_2O_2 process consumes more electrical energy whereas the consumption for the photo-Fenton process is the least one in both dyes. The electrical energy consumption for both dyes is in the following order UV/H_2O_2 > UV/TiO_2 > UV/H_2O_2/Fe^{2+}. The higher electrical energy consumption means lower process efficiency. In photo-Fenton process, the decolourisation is mainly due to Fenton reaction (ferrous ion and hydrogen peroxide) and light-induced radical pathway play a minor role in decolourisation hence, photo-Fenton process consumed lower electrical power than the other processes. The electrical energy consumption difference between UV/TiO_2 and UV/H_2O_2 process is mainly due to its difference in light absorption behavior of TiO_2 and H_2O_2 in the range of 300–400 nm. As we discussed earlier, hydrogen peroxide poorly absorbs UV light in this wavelength range. However, at this range TiO_2 absorbs it strongly. Hence, UV/H_2O_2 process consumed more electrical energy than UV/TiO_2 process. The E_{Eo} values revealed that increase of rate constant lowers the consumption of electrical energy. In UV/H_2O_2 and UV/H_2O_2/Fe^{2+} processes, RY14 dye consumes more electrical energy than RO4 dye. However, in UV/TiO_2 process RO4 decolourisation consumes more energy than RY14 dye.

3.3. Quantum yield calculation

The efficiency of the photochemical reaction (quantum yield) has been calculated for the three AOPs. The quantum yield of a reaction is defined as the number of RO4 molecules being decomposed (decolourised) per photon absorbed. (Eq. (7)).

$$\Phi = \frac{\text{Number of molecules decomposed}}{\text{Number of photons of light absorbed}} \qquad (8)$$

The photo decolourisation rate constants (k') of RO4 and RY14 dyes under the monochromatic light source can also be used for the calculation of its reaction quantum yield using Eq. (8) [21,22].

$$\Phi = \frac{k'}{2.303 I_{O,\lambda} \varepsilon_{D,\lambda} l} \qquad (9)$$

where Φ is the reaction of quantum yield (dimensionless), I_0 is the light intensity of the incident light at 365 nm (1.38×10^{-06} Einstein 1^{-1} S^{-1}), $\varepsilon_{D,\lambda}$ is the molar absorptivity of RO4 at 489 nm (2.36×10^4 cm^{-1} M^{-1}) and RY14 at 410 nm (1.3×10^4 cm^{-1} M^{-1}), l is the path length of reaction tube and it is 24 cm for 50 mL of irradiated solution.

The results of decolourisation quantum yields by the three AOPs are shown in Table 1. Obviously, the obtained quantum yield values show that the Photocatalytic and photochemical decolourisation of both dyes in all three processes seem to be slow. The quantum yield of a process decreases when the initial

Table 1
The quantum yield of RO4 and RY14 dyes at various concentrations by AOPs

Initial dye concentration ($\times 10^{-4}$)	RO4 quantum yield (Φ)			RY14 quantum yield (Φ)		
	UV/TiO_2	UV/H_2O_2	$UV/H_2O_2/Fe^{2+}$	UV/TiO_2	UV/H_2O_2	$UV/H_2O_2/Fe^{2+}$
1	0.1938	0.0305	0.0555	0.3479	0.0351	0.1176
2	0.1094	0.0194	0.0527	0.1862	0.0242	0.0879
3	0.0880	0.0186	0.0513	0.1108	0.0191	0.0762
5	0.0284	0.0070	0.0433	0.0683	0.0153	0.0634

UV/TiO_2 process: $TiO_2 = 4g/1$, pH 4.8, $I_0 = 1.38 \times 10^{-06}$ Einstein $L^{-1} S^{-1}$, UV/H_2O_2 process: $[H_2O_2] = 10$ mM, pH 3.0, $I_0 = 1.38 \times 10^{-06}$ Einstein $L^{-1} S^{-1}$, UV/ H_2O_2/Fe^{2+} process: $[H_2O_2] = 10$ mM, $[Fe^{2+}] = 0.05$ mM, pH 3.0, $I_0 = 1.38 \times 10^{-06}$ Einstein $L^{-1} S^{-1}$.

concentration of dye increases. In RO4 dye, when the concentration increases from 1×10^{-4} to 5×10^{-4} mol/L, the quantum yield decreases by 6.82, 4.35, and 1.38-fold in UV/TiO_2, UV/H_2O_2, and $Fe^{2+}/H_2O_2/UV$ processes, respectively. These results indicate that the quantum yield of UV/TiO_2 process is heavily influenced by the initial dye concentration, whereas in photo-Fenton process the influence of initial dye concentration is minimum. This appreciable difference in these two processes is mainly due to the difference in mechanism. UV light plays an important role in the UV/TiO_2 process, whereas in photo-Fenton process, the role of UV light is limited and hence, initial dye concentration affects UV/TiO_2 process more than photo-Fenton process. Another interesting result is noticed in these two processes at low and high initial concentrations. At low initial concentration (1×10^{-4} mol/L) the quantum yield of UV/TiO_2 process ($\Phi = 0.1938$) is 3.49-fold more efficient than photo-Fenton process ($\Phi = 0.0555$). However, at high initial concentration (5×10^{-4} mol/L) photo-Fenton process ($\Phi = 0.0433$) is 1.52-fold more efficient than UV/TiO_2 ($\Phi = 0.0284$) process. UV/H_2O_2 process is less efficient than UV/TiO_2 and $UV/H_2O_2/Fe^{2+}$ processes at low and high initial concentrations. A similar trend is also observed in RY14 dye. In RY14 dye, UV/TiO_2 ($\Phi = 0.3479$) process is 2.95-fold more efficient than photo-Fenton process ($\Phi = 0.1176$) at low initial concentration, whereas at high initial concentration the quantum efficiencies ($\Phi = 0.0683, 0.0634$) of these two processes are almost equal.

A comparison of the efficiencies in these two dyes by three AOPs reveals that the structure of the dye is also related to quantum yield of a process. Unambiguously, the quantum yield of RY14 removal efficiency is more than RO4 dye in all the three processes at both low and high initial concentrations. About 1.79, 1.15, and 2.11-fold higher at low initial concentration (1×10^{-4} mol/L) and 2.40, 2.18 and 1.46-fold higher at 5×10^{-4} mol/L initial concentration are observed in RY14 than RO4 with UV/TiO_2, $UV/H_2O_2 Fe^{2+}$ and UV/H_2O_2 processes respectively. In conclusion, UV/TiO_2 process is efficient if the process is operated at low initial concentrations and photo-Fenton process is efficient at higher dye concentration.

4. Conclusions

AOPs using UV light with TiO_2, H_2O_2, and H_2O_2/Fe^{2+} can effectively decolourise RO4 and RY14 dye. Photo-Fenton process is found to be most efficient in decolourisation of both dyes.

Due to poor absorption of 365 nm of UV light by hydrogen peroxide, the UV/H_2O_2 process is least efficient. The figures of merit E_{Eo} of two dyes suggest that the structure of dye molecules affect the E_{Eo} values and the electrical energy consumption is in the following order: $UV/H_2O_2 > UV/TiO_2 > Fe^{2+}/H_2O_2/UV$. In photo-Fenton process the decolourisation occurs mainly due to Fenton reaction and hence, the consumption of electrical energy is low in this process. The quantum yield values indicate that the processes with higher rate constant lead to higher quantum yields. At low initial dye concentrations the order of quantum efficiencies is $UV/TiO_2 > Fe^{2+}/H_2O_2UV > UV/H_2O_2$ in both dyes. However, at high initial dye concentrations the order is $Fe^{2+}/H_2O_2UV > UV/TiO_2 > UV/H_2O_2$ in RO4 dye and $UV/TiO_2 \approx Fe^{2+}/H_2O_2UV > UV/H_2O_2$ in RY14. It is found that photo-Fenton process is the most efficient process with respect to electrical energy consumption and photocatalytic process is most efficient, according to the quantum yield, for both dyes. The results will be useful for the design and selection of industrial scale batch reactors based on these three processes for the treatment of dye industrial wastewater.

References

[1] A.L. Pruden, D.F. Ollis, Photoassisted heterogeneous catalysis: the degradation of trichloroethylene in water, J. Catal. 82 (1983) 404–417.

[2] S. Irmak, E. Kusvuran, O. Erbatur, Degradation of 4-chloro-2-methylphenol in aqueous solution by UV irradiation in the presence of titanium dioxide, Appl. Catal. B Environ. 54 (2004) 85–91.

[3] Y. Wang, Solar photocatalytic degradation of eight commercial dyes in TiO_2 suspension, Water Res. 34 (2000) 990–994.

[4] C. Bauer, P. Jacques, A. Kalt, Photooxidation of an azo dye induced by visible light incident on the surface of TiO_2, J. Photochem. Photobiol. A 140 (2001) 87–92.

[5] M. Saquib, M. Muneer, TiO_2 mediated photocatalytic degradation of a triphenylmethane dye (gentian violet), in aqueous suspensions, Dyes Pigments 56 (2003) 37–49.

[6] I.K. Konstantinou, T.A. Albanis, TiO_2-assisted photocatalytic degradation of azo dyes in aqueous solution: kinetic and mechanistic investigations: a review, Appl. Catal. B Environ. 49 (2004) 1–14.

[7] S.F. Kang, C.H. Liao, S.T. Po, Decolorization of textile wastewater by photo-Fenton oxidation technology, Chemosphere 41 (2000) 1287–1297.

[8] S.M. Kim, A. Vogelphohl, Degradation of organic pollutants by the photo-Fenton process, Chem. Eng. Technol. 21 (1998) 187–191.

[9] G. Ruppert, R. Bauer, The photo-Fenton reaction-an effective photochemical wastewater treatment process, J. Photochem. Photobiol. A 73 (1993) 75–78.

[10] J.J. Pignatello, Dark and photoassisted Fe^{3+}-catalyzed degradation of chlorophenoxy herbicides by hydrogen peroxide, Environ. Sci. Technol. 26 (1992) 944–951.

[11] N.H. Ince, M.I. Stephen, J.R. Bolton, UV/H_2O_2 degradation and toxicity reduction of textile azo dyes, J. Adv. Oxid. Technol. 2 (1997) 442–448.

[12] N.H. Ince, D.T. Gonenc, Treatability of a textile azo dye by UV/H_2O_2, Environ. Technol. 18 (1997) 179–185.

[13] D. Georgiou, P. Melidis, A. Aivasidis, K. Gimouhopoulos, Degradation of azo-reactive dyes by ultraviolet radiation in the presence of hydrogen peroxide, Dyes Pigments 52 (2002) 69–78.

[14] A. Mohey El-Dein, J.A. Libra, U. Wiesmann, Mechanism, Kinetic model for the decolourisation of the azo dye Reactive Black 5 by hydrogen peroxide and UV-radiation, Chemosphere 52 (2003) 1069–1077.

[15] G.M. Colonna, T. Caronna, B. Marcandalli, Oxidative degradation of dyes by ultraviolet radiation in the presence of hydrogen peroxide, Dyes Pigments 41 (1999) 211–220.

[16] M. Neamtu, I. Siminiceanu, A. Yediler, A. Kettrup, Kinetics of decolourization and mineralization of reactive azo dyes in aqueous solution by the UV/H_2O_2 oxidation, Dyes Pigments 53 (2001) 93–99.

[17] A.M.L. Marechal, Y.M. Slokar, T. Taufer, Decoloration of chlorotriazine reactive azo dyes with H_2O_2/UV, Dyes Pigments 33 (1997) 281–298.

[18] R.G. Zepp, B.C. Faust, J. Hoigne, Hydroxyl radical formation in aqueous reactions (pH 3–8) of iron(II) with hydrogen peroxide: the photo-fenton reaction, Environ. Sci. Technol. 26 (1992) 313–319.

[19] D. Salari, N. Daneshvar, F. Aghazadeh, A.R. Khataee, Application of artificial neural networks for modeling of the treatnment of wastewater contaminated with methyl *tert*-butyl ether (MTBE) by UV/H_2O_2 process, J. Hazard. Mater. 125 (2005) 205–206.

[20] Calgon Carbon Corporation, The AOT Handbook, vol. 1, 1996 (Chapter 4.10).

[21] C.C. Wong Chu, The direct photolysis and photocatalytic degradation of alachlor at different TiO_2 and UV sources, Chemosphere 50 (2003) 981–987.

[22] W. Chu, Modeling the quantum yields of herbicide 2, 4-D decay in UV/H_2O_2 process, Chemosphere 44 (2001) 935–941.